Published in final edited form as:
J Mech Behav Biomed Mater. 2012 July ; 11: 112–122. doi:10.1016/j.jmbbm.2011.08.014.

Resveratrol Effect on Osteogenic Differentiation of Rat and Human Adipose Derived Stem Cells in a 3-D Culture Environment

Christopher R. Dosier[1,*], **Christopher P. Erdman**[1], **Jung Hwa Park**[2], **Zvi Schwartz**[1], **Barbara D. Boyan**[1], and **Robert E. Guldberg**[1]

[1]Parker H. Petit Institute for Bioengineering and Bioscience, Georgia Institute of Technology, 315 Ferst Drive NW, Atlanta, GA 30332

[2]School of Materials Science and Engineering, Georgia Institute of Technology, 771 Ferst Drive NW, Atlanta, GA 30332

Abstract

The goal of this study was to investigate the effect of resveratrol treatment on the osteogenic potential of human and rat adipose derived stem cells in a 3-D culture environment. Adipose derived stem cells (ADSCs) have been widely studied and have shown promise as a potential source of osteogenic progenitor cells. Previous work had investigated the effect of 25 μM resveratrol on the osteogenic differentiation of rat ADSCs in a 3-D environment and found that pre-treating cells for one passage prior to seeding on the scaffold yielded significantly more mineralization than untreated cells. We first sought to investigate whether this result was also observable with human ADSCs and found that the human cells did not respond to 25 μM resveratrol in a positive manner suggesting a species specific difference in resveratrol dosage. Therefore we next investigated multiple doses at or below 25 μM resveratrol for both rat and human ADSCs. We found that doses below 25 μM caused significantly more mineralization than 0 (untreated) and 25 μM treated cells in a 3-D culture environment. Further, we observed species differences in the total amount of mineralized matrix, as well as the mean mineral density suggesting that the nature of mineralization of the extracellular matrix was different between species. Histological examination of the scaffolds showed that the human cell constructs remain highly cellular in nature with small pockets of mineralization; while rat cell constructs showed much larger and more mature mineralized nodules. Taken together we demonstrate dose dependent differences in the mineralization response of human and rat ADSCs to resveratrol treatment, suggesting that in vitro pre-conditioning of 3D adipose-derived stem cell constructs may be an effective strategy to promote osteogenic differentiation prior to implantation.

Keywords

Adipose derived stem cells; Enrichment; Resveratrol; Mesenchymal stem cells; Micro-CT; Tissue engineering PCL scaffolds; 3D cell culture

Address for Correspondence: Robert E. Guldberg, Ph.D., Parker H. Petit Institute for Bioengineering and Bioscience, Georgia Institute of Technology, 315 Ferst Drive NW, Atlanta, GA 30332, robert.guldberg@me.gatech.edu.

1. INTRODUCTION

Adipose derived stem cells (ADSCs) were first identified in 2001 as a potential cell source for tissue engineering applications. Zuk, et al. first characterized the cells and noted that the cells were able to undergo differentiation down the mesodermal lineages including the adipogenic, osteogenic, myogenic, and chondrogenic lineages (Zuk, Zhu et al. 2001; Zuk, Zhu et al. 2002). Compared to the more widely studied mesenchymal stem cells (MSCs) from bone marrow, adipose derived stem cells showed a similar cell marker expression profile staining positive for the cell markers CD29, CD44, CD73, CD90, CD105; while negative for endothelial cell markers CD34 and CD45 (Gimble and Guilak 2003). When cultured in osteogenic media, ADSCs showed up-regulation of mRNAs for the osteogenic genes CBFα-1 and osteocalcin, and had increased alkaline phosphatase activity compared to cells in control media in standard 2-D culture (Hattori, Sato et al. 2004; Schaffler and Buchler 2007). Knippenberg later showed that ADSCs cultured in the presence of bone morphogenetic protein 2 (BMP-2) and BMP-7 showed greater osteogenic differentiation in terms of alkaline phosphatase activity compared to controls in standard 2-D culture (Knippenberg, Helder et al. 2006). Moreover, a major advantage of ADSCs is their relative abundance as well as their faster proliferation rate compared to bone marrow MSCs and this allows for more rapid expansion to obtain clinically relevant cell numbers compared to MSCs (Cowan, Shi et al. 2004; Fraser, Wulur et al. 2006; Nakagami, Morishita et al. 2006).

Bone tissue engineering research using adipose derived stem cells has been limited with mixed outcomes and mainly focused on orthopaedic defects in animal models, e.g. calvarial defects as well as defects in the radius and tibia (Niemeyer, Fechner et al. 2010; Rhee, Ji et al. 2010). Cowan showed that implantation of juvenile and adult ADSCs harvested from rats led to greater bone formation in a critically sized calvarial defect compared to untreated controls (Cowan, Shi et al. 2004). Niemeyer investigated the use of ADSCs in a tibial bone defect model and demonstrated that when undifferentiated ADSCs were implanted, little bone was formed. Moreover, the ADSCs differentiated down the adipogenic lineage as evidenced histologically by the presence of lipid filled vacuoles in the defect site (Niemeyer, Fechner et al. 2010). However, a recent report in which ADSCs were transduced with a BMP-2 plasmid-containing adenovirus showed complete healing of a radial defect in rabbits 12 weeks post-implantation (Wei Hao 2009).

These conflicting reports demonstrate a critical criterion for the implantation of ADSCs for bone tissue engineering in that they appear to require a degree of cell differentiation to direct the behavior of the cells in vivo. This is particularly relevant for ADSCs, since upon isolation the cell population consists of multiple cell types including osteoprogenitor cells, pre-adipocytes, and vascular smooth muscle cells (Gimble and Guilak 2003). Further, the cells may be more prone to undergo adipogenic differentiation considering the source of the cells is adipose tissue. Therefore, a method of selecting and enriching the population of adipose derived stem cells for osteoprogenitors would be advantageous for bone tissue engineering applications.

While gene therapy via viral transduction is a widely studied technique for controlling cell behavior, this has several drawbacks in terms of clinical translation. A pharmacological approach would provide a simpler method to promote differentiation along a given lineage. Resveratrol is one such pharmacological agent and has been shown to have a variety of physiologic functions including estrogenic activity, anti-inflammatory activity, vaso-relaxation effects, anti-cancer activity, as well as modulation of lipid metabolism (Fremont 2000). Further, reports have shown that resveratrol is able to modulate both osteogenesis and adipogenesis (Rayalam, Della-Fera et al. 2011; Tseng, Hou et al. 2011). This appears to be caused by stimulating the Sirt1 pathway, which simultaneously promotes osteogenic

differentiation and inhibits adipogenic differentiation. Thus, adipogenesis is down regulated in the presence of resveratrol by inhibition of PPAR-γ, a key player in the control of both osteogenic and adipogenic differentiation (Shockley, Lazarenko et al. 2009). Further, studies have shown that resveratrol treatment of mouse MSCs promoted osteogenic differentiation due to up-regulation of the Sirt1 pathway (Boissy, Andersen et al. 2005; Backesjo, Li et al. 2006; Costa, Rohden et al. 2011). A recent report demonstrated that the increase in the osteogenic differentiation of resveratrol treated ADSCs may be due to downstream interaction with the promoter region of the Runx-2 protein, a key player in osteogenic differentiation of adult stem cells (Tseng, Hou et al. 2011). These data demonstrate that resveratrol is a good candidate to promote osteogenic differentiation while simultaneously inhibiting adipogenesis in ADSCs and may therefore promote mineralization of ADSCs for bone tissue engineering purposes.

We have previously shown that resveratrol can promote 3-D osteogenic differentiation on PCL/collagen scaffolds of rat ADSCs (rADSCs) via enrichment of the cell source for osteoprogenitor cells. The PCL/collagen system provides an effective test-bed for evaluating osteogenic differentiation in a 3-D culture environment, with the PCL providing a consistent porosity and the collagen facilitating cell adhesion and retention to the scaffold. Pre-treatment of the rADSCs with 25 μM resveratrol resulted in greater amounts of mineralized matrix on the PCL/collagen scaffold than untreated cells (Erdman, Dosier et al. 2011). Further, continuous treatment did not result in any enhanced mineralized matrix formation compared to untreated or pre-treated cells, demonstrating that short exposure to resveratrol is sufficient to induce a beneficial effect on osteogenic differentiation.

The aim of this study was to determine whether similar beneficial effects were observable in human ADSC populations. We further investigated the effect of resveratrol dosage on the 3-D osteogenic differentiation of both rat and human ADSCs in terms of mineral volume produced as well as mean density of the mineralized matrix. We next performed a histological evaluation of the scaffolds after mineralization to investigate differences in the nature of mineral deposition in the extra cellular matrix. Finally, we analyzed the surface and chemical makeup of mineralized constructs using scanning electron microscopy (SEM), x-ray photoelectron spectroscopy (XPS), and thermogravimetric (TGA) analyses.

2. METHODS

2.1 Cell Isolation and Culture

2.1.1 Rat ADSC Cell Isolation—Inguinal fat pads, which are subcutaneous fat surrounding the thigh were harvested from multiple 100–125g male Sprague-Dawley rats (Harlan, Indianapolis, IN) bilaterally according to a protocol approved by the Institutional Animal Care and Use Committee at Georgia Institute of Technology and the US Army Medical Research and Materiel Command Animal Care and Use Review Office. Briefly, the tissue was pooled and washed three times in Hank's balanced saline solution (HBSS), and digested in 0.25% trypsin for 30 minutes at 37 C. The tissue was then cut into smaller pieces and digested in 9125 units of collagenase IA (Sigma, St. Louis, MO) and 75 units of dispase (Gibco, Invitrogen, Carlsbad, CA) for three hours. The upper layer of adipocytes was removed, and the cell suspension was filtered through a 40μm cell strainer. The digestion was stopped with MSC growth media (GM) (Lonza, Basel, Switzerland), which contains fetal bovine serum, and the cells were collected by centrifugation. The cells were plated at 5,000 cells/cm^2 in T-75 flasks. Cultures were washed twice with phosphate buffered saline (PBS) and fed with GM at 24 and 48 hours after plating. Cell expansion was performed in which cells were grown to sub-confluence and then trypsinized and reseeded for 2 passages prior to being cryo-preserved.

2.1.2 Human ADSC Cell Isolation—Adipose tissue from an adolescent donor was obtained from the Children's Hospital Atlanta and cells were isolated and cultured as described above. The obtaining and processing of the tissue was performed according to Georgia Institute of Technology Institute Review Board protocol H08244.

2.2 2-D Human ADSC Culture and Characterization

2.2.1 Cell Culture—Passage 2 hADSCs were thawed and cultured in T75 flasks in GM (Lonza). At 80% confluence the cells were passaged and plated at 5000 cells/cm2 in GM. Starting the following day, the ADSCs were then treated for 7 days with 0, 6.25, 12.5, and 25μM resveratrol in GM. Media were changed every 48 hours.

2.2.2 Osteogenic Differentiation Markers—Twenty-four hours prior to harvest, the media were replaced with fresh medium with and without resveratrol. At harvest the conditioned media were collected, and the cells were lysed with 0.05% Triton-X 100, 10 second sonication, and one freeze-thaw cycle. Alkaline phosphatase (ALP) specific activity was measured in cell lysates as the release of p-nitrophenol from p-nitrophenylphosphate at pH 10.25. Protein levels were measured with a BCA protein assay kit (Pierce, Rockford, IL). Osteocalcin levels in the conditioned media were measured via the Human Osteocalcin Radioimmunoassay kit (Biomedical Technologies, Stoughton, MA). Osteoprotegerin (OPG) levels in the conditioned media were measured via the Osteoprotegerin ELISA (R&D Systems, Minneapolis, MN). Osteocalcin and osteoprotegerin assays were each run according to manufacturer's instructions and levels were normalized to DNA levels, quantified with picogreen florescence in the cell lysate (Invitrogen).

2.3 PCL/Collagen 3-D Scaffold Preparation

PCL scaffolds were prepared as described previously (Peister, Deutsch et al. 2009). Briefly, 100×100×9 mm sheets of medical grade poly ε-caprolactone (PCL, Osteopore International, Singapore) with 85% porosity were cut with a 5 mm diameter biopsy punch to yield a cylindrical scaffold. The scaffolds were then briefly treated with 5M sodium hydroxide to roughen the surface and facilitate cell attachment. Scaffolds were then washed three times with sterile water and sterilized overnight via 70% ethanol evaporation. Sterile PCL scaffolds were washed with excess sterile water three times and placed into a custom mold. Rat tail collagen type I (Trevigen, Gaithersburg, MD) was diluted with 0.05% acetic acid to 1.5 mg/mL, neutralized with 1M sodium bicarbonate, and aseptically pipetted into the mold to occlude the pores of the scaffold. The scaffold/collagen gel constructs were then placed in a −80°C freezer for 1 hour prior to being lyophilized overnight. Lyophilized scaffolds were placed in a sterile scaffold holder and into 24-well low-attachment cell culture plates (Corning, Lowell, MA) and stored until cell seeding.

2.4 Treatment Regimen Effect on hADSC Osteogenic Differentiation

Cryo-preserved cells were thawed and plated for 24 hours. Cells were then trypsinized and plated at a density of 250 cells/cm^2 and cultured for one week in GM. One half of the cultures were treated with 25μM resveratrol every two days. Cells were harvested, counted, and reconstituted at a density of 3×10^4 cells/μL. 100μL (3×10^6) of cells were then carefully pipetted onto the tops of the scaffold/collagen constructs and allowed to attach to the surface. After a 1-hour incubation, GM was added to the culture wells so that the cell-scaffold constructs were completely submerged in media. After 48 hours media were changed to osteogenic differentiation media consisting of α-MEM (Invitrogen) supplemented with 16% FBS (Atlanta Biologics, Lawrenceville, GA), 1% penicillin-streptomycin (Invitrogen), 50 μg/mL ascorbic acid 2-phosphate (Sigma), 50 ng/mL thyroxine (Sigma), 6 mM beta-glycerophosphate (Sigma), and 1 nM dexamethasone

(Sigma). Cell/scaffold constructs on the continuous resveratrol treatment regimen were given the osteogenic differentiation medium supplemented with 25μM resveratrol. Media were changed twice weekly during culture on the 3D scaffolds. Scaffolds were placed in a custom holder consisting of a plastic disk with four stainless steel pins, and cultured in a 24-well low-attachment cell culture plate. Cells were cultured dynamically on an orbital shaker (Stovall Life Scientific, Greensboro, NC) at a rate of 6.5 RPM in a CO2 incubator.

2.5 Cell Distribution and Seeding Efficiency in 3D Environment

Cell/scaffold constructs were harvested 24 hours after seeding. Scaffolds were bisected. A live/dead assay was performed on one half with the LIVE-DEAD Viability/Cytotoxicity kit (Invitrogen, Eugene, Oregon). Qualitative distribution of the cells throughout the scaffold was observed via fluorescent microscopy using a Zeiss Axio Observer (G ttingen, Germany) microscope at 4× magnification. Non-attached cells were collected from the media samples 24 hours after seeding and DNA quantified. The number of cells on the scaffold was determined using the Pico Green DNA assay (Invitrogen) together with a cell ladder. Cell numbers were then normalized to the number of cells delivered.

2.6 Dose Dependent Resveratrol Pre-treatment of Rat and Human ADSCs

Cryo-preserved cells were thawed and plated for 24 hours. Cells were then trypsinized and plated at a density of 250 cells/cm^2 and cultured for one week in GM, GM supplemented with 6.25 μM resveratrol, 12.5 μM resveratrol, or 25 μM resveratrol. Cells were grown for one passage and trypsinized at sub-confluence. Cells were then harvested and seeded onto PCL/collagen scaffolds described in 2.3 and placed in osteogenic media after 48 hours and cultured on an orbital shaker. Micro-CT imaging was performed at 4, 8 and 12 weeks as described previously. At the end of 12 weeks, 3 scaffolds of each group were fixed in 10% neutral buffered formalin for 48 hours and then evaluated histologically. The remaining samples were used for fluorescent imaging.

2.7 Micro-CT Imaging

At 4, 8, and 12 weeks, cell scaffold constructs were aseptically removed from culture and placed in custom tubes for Micro-CT scanning. Mineralized matrix of the cell/scaffold constructs was determined by using a VivaCT scanner (Scanco Medical, Brüttisellen, Switzerland) at 55 kVp, 109 mA, 1024 mu scaling, and a 200 ms integration time. The constructs were evaluated with a lower threshold of 80 with a filter width of 1.2 and a filter support of 1.0. The total volume of the mineralized matrix as well as the mean mineral density of the mineralized nodules was determined.

2.8 Fluorescent Imaging and Histological Evaluation

Fluorescent imaging was performed on scaffolds following 24 hours of culture. Scaffolds were washed with PBS thrice and then sectioned longitudinally and stained with calcein and ethidium and imaged using a Zeiss Axio Observer (G ttingen, Germany) microscope at 4× magnification. Fixed samples were sectioned longitudinally and von Kossa staining for mineralized matrix was performed. Gross images of the cell/scaffold constructs were then taken using a camera.

2.9 Surface Characterization and SEM Imaging

The surface morphology of PCL, PCL/Col, PCL/Col-hADSCs, and PCL/Col-rADSCs was obtained by using a Hitachi S-3700 VP-scanning electron microscope (Hitachi high technologies America, Inc., USA) with an accelerating voltage of 15 kV. Elemental distribution of the substrates used in this study was analyzed by using the energy-dispersive x-ray spectroscopy (EDX) detector attached to the Hitachi S-3700N VP-SEM. In order to

determine organic and inorganic contents of PCL, PCL/Col, PCL/Col-hADSCs, and PCL/Col-rADSCs, thermogravimetric analyses (TGA) were performed under nitrogen using a TA Instruments Q50 Thermogravimetric Analyzer (Delaware, USA). Substrates weighing approximately 10 – 30 mg were heated from 25 °C to 800 °C at a rate of 10 °C/minute and the weight loss percentage of each substrate are reported. The surface chemical composition and chemical mapping were carried out by using x-ray photoelectron spectroscopy (XPS; Thermo K-Alpha, Thermo Fisher Scientific Inc., MA, USA). The XPS analysis was performed under ultra high vacuum (less than 10^{-9} Torr) with a monochromatic Al Kα X-ray source ($h\nu$ = 1486.6 eV, 90° take-off angle). Thermo Advantage 4.43 software package (Thermo Fisher Scientific, Inc.) was used to evaluate the XPS spectra.

2.9 Statistical Analysis

Data were analyzed with a one-way ANOVA followed by a t-test with a Bonferroni's modification. 2-D experiments had an n=6 and 3-D experiments had an n=5.

3. RESULTS

3.1 2-D Osteogenic Differentiation

Resveratrol treatment had a dose-dependent effect on hADSC cell count with progressively less DNA with increase in resveratrol dose (Figure 1A). Resveratrol treatment had an effect on alkaline phosphatase specific activity with increased enzyme activity in hADSCs until 25μM, at which point activity decreased (Figure 1B). Resveratrol increased osteocalcin levels in hADSCs in a dose-dependent manner (Figure 1C). Osteoprotegerin levels were also elevated over control for the hADSCs for all doses. No dosage differences were observed for osteoprotegerin in resveratrol treated cells (Figure 1D).

3.2 hADSC Cell Distribution and Seeding Efficiency on PCL/Collagen Scaffolds

Live/Dead imaging showed high cell attachment and viability for both groups. Cells were readily observable attached to the struts of the scaffold as well as forming cell/collagen networks that span in between the struts of the scaffold (Figure 2A). This was confirmed by measuring the seeding efficiency via pico Green DNA assay. Cells that were pre-treated with 25 μM resveratrol had a seeding efficiency of 97.6±.4% while untreated cells had a 97.5±.9% of cells seeded.

3.3 25 μM Resveratrol Pre-treatment and Continuous Treatment on hADSC Mineralization

Human ADSCs readily produce mineral on the PCL/collagen scaffolds in the presence of osteogenic media as shown in Figure 2B, C, and D. At all time points, resveratrol pre-treatment (25 μM) resulted in significantly less mineralization than untreated cells. Continuous resveratrol treatment (osteogenic media + 25 μM resveratrol) further reduced mineralized matrix at all time points. It should be noted that at each successive time point there was a significant increase in mineralized matrix compared to the previous time point for each group respectively.

3.4 Dose Dependent Effect of Resveratrol on hADSC and rADSC Osteogenic Differentiation

Micro-CT imaging demonstrated that at 4 weeks all groups of hADSCs were mineralizing throughout the entirety of the scaffold (Figure 3A). At 4 weeks, the 12.5 μM group had significantly greater mineral volume than the 25 μM group, indicating that a high dose of reseveratrol reverses its promotion of mineralization seen in lower dose groups (Figure 3B). The 12.5 μM group also approached significance compared to the 0 μM (untreated) group although it was not statistically significant. By 8 weeks, all groups continued to mineralize with their matrix volume being significantly higher than the 4 week time point. Interestingly,

by 8 weeks the 6.25 μM group displayed the greatest amount of mineralized matrix and was significantly higher than the 25 μM group (Figure 3C). Similar results were observed at 12 weeks, with a significant increase in mineralization of all groups compared to the 8 week time point (Figure 3D). These data demonstrate that for resveratrol doses lower than 25 μM, pre-treatment of resveratrol is sufficient to increase mineralization of human ADSCs with higher doses promoting greater mineralization at early time points, and lower doses promoting greater mineralization at later time points.

Mineralization of rat ADSCs was robust in all treatment groups as seen on the representative Micro-CT images (Figure 4A). Quantification of the mineralized matrix showed that at 4 weeks the 12.5 μM group significantly increased the mineral volume compared to the 0 μM group (Figure 4B). Similar results were observed at 8 weeks with both the 6.25 μM and 12.5 μM groups having more mineralized matrix than the 0 and 25 μM groups (Figure 4C). By 12 weeks the 6.25 μM group was significantly higher than all other dosage groups (Figure 4D). At all time points the mineralization increased compared to the previous time point for all resveratrol dosages. It should also be noted that the rat ADSC groups all produced more mineralized matrix than the corresponding human ADSC groups at all time points.

3.5 hADSC and rADSC Mean Density of Mineralized Matrix

Quantification of the mean density of the mineralized nodules showed that at 4 weeks rat and human ADSC constructs showed similar mineral density with only the 25uM groups being significantly different (Figure 5A). However at 8 and 12 weeks there were significant differences in the mean density with rat cells showing higher mean density compared to human cells at all doses (Figure 5B and 5C). Interestingly, rat ADSC constructs increased in mean density significantly over time for all groups from 4 to 8 weeks. From 8 to 12 weeks the middle two doses were significantly different from the previous time point although all groups increased in mean density. At all time points human cells had a relatively consistent mean density regardless of resveratrol dose. Some groups did significantly increase over time, but the increases were lower than observed for the rADSCs.

3.6 Histological Analysis of Mineralized Matrix of hADSC and rADSC Constructs

Cell scaffold constructs from both species were sectioned longitudinally through the middle of the construct and calcein and ethidium imaging of the mineralized matrix was performed. Rat ADSC groups displayed large nodules of mineral with live cells being found on top of the mineralized nodules as well as on the struts of the scaffold (Figure 6A). Human ADSC constructs showed similar results with similar mineralized nodules (Figure 6B), however there were also large areas of confluent cells that were not observed in the rat ADSC constructs (Figure 6C). Von Kossa staining showed that both human and rat cell constructs had large deposits of mineral (Figure 6D and 6E). It should be noted that the rat cell groups stained darker and blacker than the human cell groups which had a more brownish color, confirming Micro-CT results in which the rat cell groups had denser mineral nodules than human cell groups.

3.7 Surface Examination of hADSC and rADSC Constructs

3.7.1 SEM Imaging—SEM images of the scaffold with and without mineralized cells showed distinguishing features. Similar to the fluorescent imaging results, SEM images showed that human cell constructs had much more ECM compared to rat cells, however the rat cell constructs had much larger nodules compared to the human cells (Figure 7C, D, G, & H).

3.7.2 TGA Analysis—The weight percentage of organic and inorganic contents of substrates used in this study was determined by thermogravimetric analysis (TGA). The

weight loss profile and percentage as a function of increasing temperature from 25 °C to 800 °C is shown in Figure 8A. PCL had 99.3% weight loss at 800 °C while PCL with lyophilized collagen had 98.8% weight loss. Human and rat cell mineralized constructs had 47%, and 68% weight loss, respectively. The weight loss of human bone and rat bone corresponded to 34% and 33%, respectively. PCL and PCL/Col consist of organic components while PCL/Col-hADSCs (mineralized human constructs) and PCL/Col-rADSCs (mineralized rat constructs) consisted of both organic and inorganic materials like human and rat bones.

3.7.3 XPS Analysis—The inorganic contents of PCL/Col-hADSCs and PCL/Col-rADSCs were measured by x-ray photoelectron spectroscopy (XPS). Calcium (Ca_{2p}, 347 eV) and phosphorous (P_{2p}, 133 eV) peaks were detected in human bone, PCL/Col-hADSCs, rat bone, and PCL/Col-rADSCs, however these two peaks were not observed on PCL and PCL/Col surfaces (Figure 8B) demonstrating that inorganic mineral deposition by human and rat cells occurred in the tissue engineered constructs.

The distribution of Ca and P on human bone, PCL/Col-hADSCs, rat bone, and PCL/Col-rADSCs surfaces was obtained by XPS chemical mapping (Figure 8C). In human bone samples, Ca and P demonstrated stronger and more widespread intensity compared to rat bones. PCL/Col-hADSCs distinctly showed that Ca and P were locally concentrated rather than evenly spread. On PCL/Col-rADSCs constructs, Ca and P were present with strong intensity and relatively well spread. The XPS mapping showed higher intensity suggesting a denser mineralized matrix for the rat cell constructs compared to the human cell constructs, confirming the mean mineral density differences we obtained from Micro-CT.

DISCUSSION

This work examines the osteogenic potential of both rat and human adipose derived stem cells in a 3-D environment as well as the impact of pharmaceutical treatment to improve the osteogenic potential of the cell source. We observed that there were species, dosage, and temporal differences in the mineralized matrix production of rADSCs and hADSCS, demonstrating that resveratrol pre-treatment is an effective means to increase the osteogenic potential of these cells. In addition, differences in the method of mineralization were observed between the two species. These data demonstrate that resveratrol pre-treatment of ADSCs results in greater mineralized matrix than untreated cells and that species should be taken into account when evaluating the osteogenic potential of cells from various sources for tissue engineering applications.

Most studies comparing cell sources from different species have focused on mesenchymal stem cells from bone marrow aspirates (Woodbury, Schwarz et al. 2000; Javazon, Colter et al. 2001; Ikeuchi, Ito et al. 2003; Osyczka, Diefenderfer et al. 2004; Zavan, Giorgi et al. 2007). Further, many studies focus on age related differences by comparing adult cells to fetal cells (De Coppi, Callegari et al. 2007; Dupont, Sharma et al. 2010). While age is an important consideration, the species from which the cell source is tested in tissue engineering models should also be considered in selecting a cell source. Such studies have been limited to examining different strains of mice (Peister, Mellad et al. 2004), and to our knowledge only one study has looked at the difference in osteogenic potential of adipose derived stem cells from different species (Ni, Zhou et al. 2009).

We show that there are differences in the osteogenic potential of the cell sources as well as dosage effects of resveratrol to improve osteogenic differentiation. Adipose derived stem cells obtained from rats showed greater mineralization at all time points compared to human cells. Further, the mean density of the nodules in rat cell constructs was higher than human

at later time points suggesting a more mature mineralization in the rat cell constructs. A possible explanation for this is the use of lyophilized rat tail collagen I in our PCL scaffold system. Rat cells may be able to assimilate the collagen I and remodel and mineralize it more efficiently than the human cells. This is supported by the differences seen at the early time point of four weeks as well as the larger mineral nodules observed in the rat cell constructs. Human cell mineralization may be altered in the presence of human collagen I and should be tested in the future. Another possible explanation for the observed differences in mineralization may be related to variations in resveratrol metabolism. Human cells and rat cells have been shown to metabolize resveratrol differently and this may influence the osteogenic differentiation of the cells (Yu, Shin et al. 2002). Further, it should be noted that the cells used in this study were isolated from different anatomical sites, and this may serve as a compounding factor to the different levels of mineralization observed.

Resveratrol has been shown to induce osteogenesis in preference to adipogenesis in mesenchymal and adipose derived stem cells (Backesjo, Li et al. 2006; Erdman, Dosier et al. 2011). Previous work in our lab demonstrated that rat adipose derived stem cells pre-treated with resveratrol produce more mineralized matrix than untreated and continuously treated cells (Erdman, Dosier et al. 2011). In this study, we extended this work to analyze human adipose derived stem cells. We observed that the human cells did not respond well to the 25 μM resveratrol dose regardless of treatment regimen. We therefore performed a dose dependency study evaluating pre-treatment with resveratrol for both human and rat adipose derived stem cells. We observed dosage differences in both rat and human cell constructs. For both rat and human cell constructs, 12.5 μM resveratrol pre-treatment resulted in greater mineralized matrix at 4 weeks. Doses higher than 12.5 μM led to decreased mineralized matrix suggesting a potentially cytotoxic effect. At later time points, a lower dose of 6.25 μM resveratrol had the greatest mineralized matrix. Taken together, this suggests that higher doses lead to more rapid differentiation and thus higher mineralized matrix initially, while lower doses promote differentiation while retaining better cell viability, resulting in greater mineralized matrix at later time points. These results suggest that the resveratrol dosage should be taken into consideration and tailored for the bone tissue engineering application. For short time course studies, a higher dose may produce the best results in terms of mineral production, and contrarily for long time course studies a lower dose may be the most beneficial.

The PCL/collagen system used in this study provides a consistent and reproducible method to evaluate the osteogenic potential of cells from a variety of sources. Our lab and others have used this to test cells from human bone marrow aspirates, amniotic fluid stem cells, mouse cells, and now adipose derived stem cells (Peister, Deutsch et al. 2009; Dupont, Sharma et al. 2010; Rai, Lin et al. 2010; Erdman, Dosier et al. 2011). An advantage of this system is the consistent porosity as each scaffold is punched from a uniform sheet of material. This eliminates the variable of poor mass transport due to varying porosity in the scaffold affecting the results. As such, any differences observed should be mainly attributable to the osteogenic potential of the cell source. When we mapped the mineral distribution of the mineralized matrix using XPS, we observed that the rat cells had higher mineral content compared to human constructs. As expected, when compared to native bone from both rats and humans however, the mineral content within the 3-D constructs was markedly lower, indicating a still immature mineralized extracellular matrix relative to bone tissue.

CONCLUSION

In this study we evaluated the osteogenic potential of human and rat adipose derived stem cells subjected to pre-treatment with resveratrol prior to seeding within 3-D tissue-

engineered constructs. We found that the dose of resveratrol has a significant effect on the mineralized matrix production of both cell sources. We further found that rat adipose derived stem cells produced a larger quantity and more mature mineralized matrix compared to the human cell constructs. Taken together we demonstrate that the species as well as resveratrol dose can have a significant effect on the mineralized matrix production of adipose derived stem cells.

Acknowledgments

This work was supported by the United States Department of Defense, NIH grant R01-AR056694, as well as the Center for Advanced Bioengineering for Soldier Survivability (CABSS) grants W81XWH-11-1-0306 and W81XWH-08-1-0704.

References

Backesjo CM, Li Y, et al. Activation of Sirt1 decreases adipocyte formation during osteoblast differentiation of mesenchymal stem cells. J Bone Miner Res. 2006; 21(7):993–1002. [PubMed: 16813520]

Boissy P, Andersen TL, et al. Resveratrol inhibits myeloma cell growth, prevents osteoclast formation, and promotes osteoblast differentiation. Cancer Res. 2005; 65(21):9943–52. [PubMed: 16267019]

Costa CD, Rohden F, et al. Resveratrol Upregulated SIRT1, FOXO1, and Adiponectin and Downregulated PPARgamma1-3 mRNA Expression in Human Visceral Adipocytes. Obes Surg. 2011

Cowan CM, Shi YY, et al. Adipose-derived adult stromal cells heal critical-size mouse calvarial defects. Nat Biotechnol. 2004; 22(5):560–7. [PubMed: 15077117]

De Coppi P, Callegari A, et al. Amniotic fluid and bone marrow derived mesenchymal stem cells can be converted to smooth muscle cells in the cryo-injured rat bladder and prevent compensatory hypertrophy of surviving smooth muscle cells. J Urol. 2007; 177(1):369–76. [PubMed: 17162093]

Dupont KM, Sharma K, et al. Human stem cell delivery for treatment of large segmental bone defects. Proc Natl Acad Sci U S A. 2010; 107(8):3305–10. [PubMed: 20133731]

Erdman CP, Dosier CR, et al. Effects of Resveratrol on Enrichment of Adipose-derived Stem Cells and their Differentiation to Osteoblasts in Two and Three Dimensional Cultures. Journal of Tissue Engineering and Regnerative Medicine. 2011 Submitted, In Press.

Fraser JK, Wulur I, et al. Fat tissue: an underappreciated source of stem cells for biotechnology. Trends Biotechnol. 2006; 24(4):150–4. [PubMed: 16488036]

Fremont L. Biological effects of resveratrol. Life Sci. 2000; 66(8):663–73. [PubMed: 10680575]

Gimble J, Guilak F. Adipose-derived adult stem cells: isolation, characterization, and differentiation potential. Cytotherapy. 2003; 5(5):362–9. [PubMed: 14578098]

Hattori H, Sato M, et al. Osteogenic potential of human adipose tissue-derived stromal cells as an alternative stem cell source. Cells Tissues Organs. 2004; 178(1):2–12. [PubMed: 15550755]

Ikeuchi M, Ito A, et al. Osteogenic differentiation of cultured rat and human bone marrow cells on the surface of zinc-releasing calcium phosphate ceramics. J Biomed Mater Res A. 2003; 67(4):1115–22. [PubMed: 14624496]

Javazon EH, Colter DC, et al. Rat marrow stromal cells are more sensitive to plating density and expand more rapidly from single-cell-derived colonies than human marrow stromal cells. Stem Cells. 2001; 19(3):219–25. [PubMed: 11359947]

Knippenberg M, Helder MN, et al. Osteogenesis versus chondrogenesis by BMP-2 and BMP-7 in adipose stem cells. Biochem Biophys Res Commun. 2006; 342(3):902–8. [PubMed: 16500625]

Nakagami H, Morishita R, et al. Adipose tissue-derived stromal cells as a novel option for regenerative cell therapy. J Atheroscler Thromb. 2006; 13(2):77–81. [PubMed: 16733294]

Ni YW, Zhou YS, et al. Comparison of biological characteristics of human, rabbit and rat adipose tissue-derived stromal cells in vitro. Beijing Da Xue Xue Bao. 2009; 41(1):95–9. [PubMed: 19221574]

Niemeyer P, Fechner K, et al. Comparison of mesenchymal stem cells from bone marrow and adipose tissue for bone regeneration in a critical size defect of the sheep tibia and the influence of platelet-rich plasma. Biomaterials. 2010; 31(13):3572–9. [PubMed: 20153047]

Osyczka AM, Diefenderfer DL, et al. Different effects of BMP-2 on marrow stromal cells from human and rat bone. Cells Tissues Organs. 2004; 176(1–3):109–19. [PubMed: 14745240]

Peister A, Deutsch ER, et al. Amniotic fluid stem cells produce robust mineral deposits on biodegradable scaffolds. Tissue Eng Part A. 2009; 15(10):3129–38. [PubMed: 19344289]

Peister A, Mellad JA, et al. Adult stem cells from bone marrow (MSCs) isolated from different strains of inbred mice vary in surface epitopes, rates of proliferation, and differentiation potential. Blood. 2004; 103(5):1662–8. [PubMed: 14592819]

Rai B, Lin JL, et al. Differences between in vitro viability and differentiation and in vivo bone-forming efficacy of human mesenchymal stem cells cultured on PCL-TCP scaffolds. Biomaterials. 2010; 31(31):7960–70. [PubMed: 20688388]

Rayalam S, Della-Fera MA, et al. Synergism between resveratrol and other phytochemicals: Implications for obesity and osteoporosis. Mol Nutr Food Res. 2011

Rhee SC, Ji YH, et al. In Vivo Evaluation of Mixtures of Uncultured Freshly Isolated Adipose-Derived Stem Cells and Demineralized Bone Matrix for Bone Regeneration in a Rat Critically Sized Calvarial Defect Model. Stem Cells Dev. 2010

Schaffler A, Buchler C. Concise review: adipose tissue-derived stromal cells--basic and clinical implications for novel cell-based therapies. Stem Cells. 2007; 25(4):818–27. [PubMed: 17420225]

Shockley KR, Lazarenko OP, et al. PPARgamma2 nuclear receptor controls multiple regulatory pathways of osteoblast differentiation from marrow mesenchymal stem cells. J Cell Biochem. 2009; 106(2):232–46. [PubMed: 19115254]

Tseng PC, Hou SM, et al. Resveratrol promotes osteogenesis of human mesenchymal stem cells by up-regulating RUNX2 gene expression via SIRT1/FOXO3A axis. J Bone Miner Res. 2011

Hao, Wei, et al. Enhanced bone formation in large segmental radial defects by combining adipose-derived stem cells expressing bone morphogenetic protein 2 with nHA/RHLC/PLA scaffold. International Orthopaedics. 2009

Woodbury D, Schwarz EJ, et al. Adult rat and human bone marrow stromal cells differentiate into neurons. J Neurosci Res. 2000; 61(4):364–70. [PubMed: 10931522]

Yu C, Shin YG, et al. Human, rat, and mouse metabolism of resveratrol. Pharm Res. 2002; 19(12): 1907–14. [PubMed: 12523673]

Zavan B, Giorgi C, et al. Osteogenic and chondrogenic differentiation: comparison of human and rat bone marrow mesenchymal stem cells cultured into polymeric scaffolds. Eur J Histochem. 2007; 51(Suppl 1):1–8. [PubMed: 17703587]

Zuk PA, Zhu M, et al. Human adipose tissue is a source of multipotent stem cells. Mol Biol Cell. 2002; 13(12):4279–95. [PubMed: 12475952]

Zuk PA, Zhu M, et al. Multilineage cells from human adipose tissue: implications for cell-based therapies. Tissue Eng. 2001; 7(2):211–28. [PubMed: 11304456]

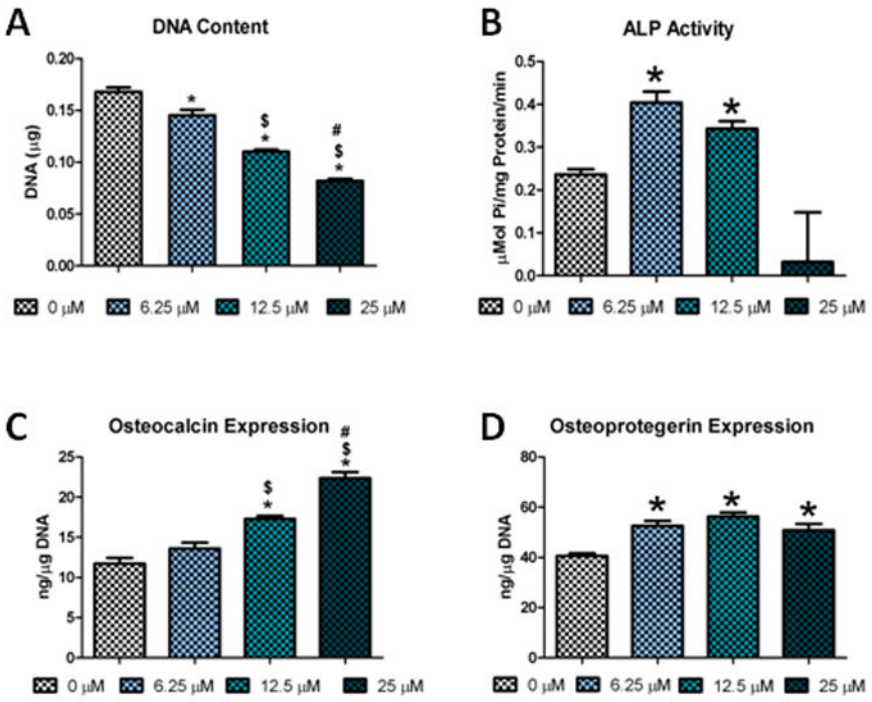

Figure 1.

Resveratrol effect on the osteogenic differentiation of hADSCs in a 2-D culture environment: A) DNA Content of 2-D cultured hADSCs; B) ALP activity after 7 days of culture in growth media; C) Osteocalcin levels; D) Osteoprotegerin levels (* = significantly different from 0 μM ($p<.05$), $ = significantly different from 6.25 μM ($p<.05$), # = significantly different from 12.5 μM ($p<.05$))

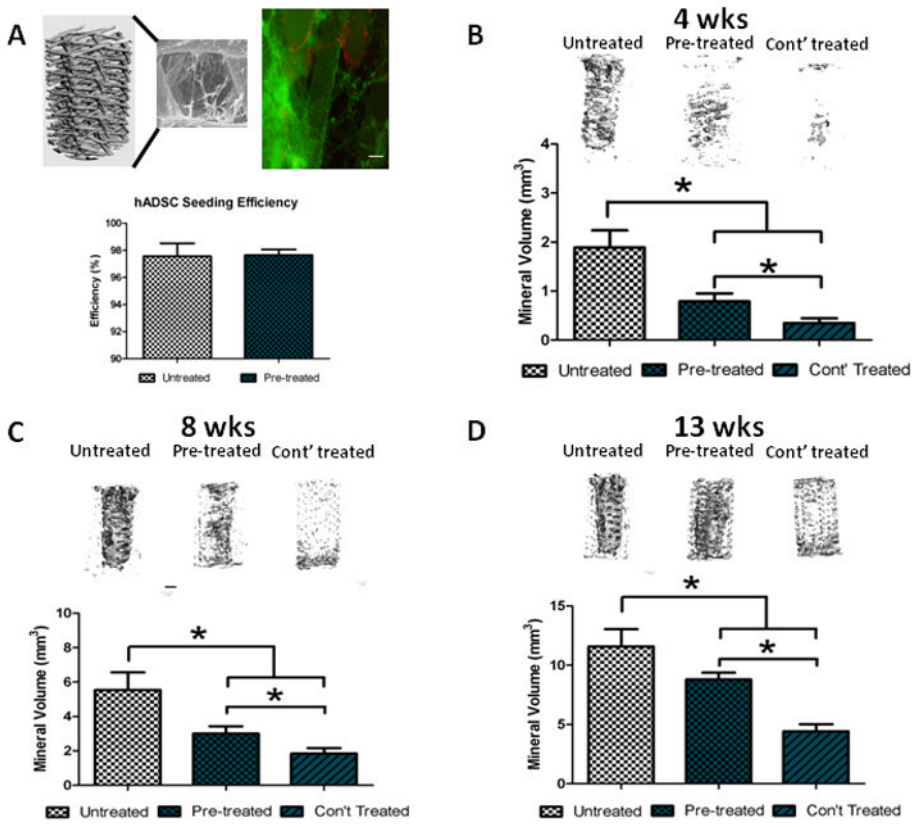

Figure 2.

The effect of resveratrol treatment regimen on the 3-D osteogenic differentiation of hADSCs: A) PCL/collagen scaffold with LIVE/DEAD stain and seeding efficiency (scale bar = .5 mm; LIVE = green, DEAD= red); Representative Micro-CT images and mineral volume for hADSCs under different treatment regimens after 4 weeks (B), 8 weeks (C), and 12 weeks (D) in osteogenic media. * = $p<.05$.

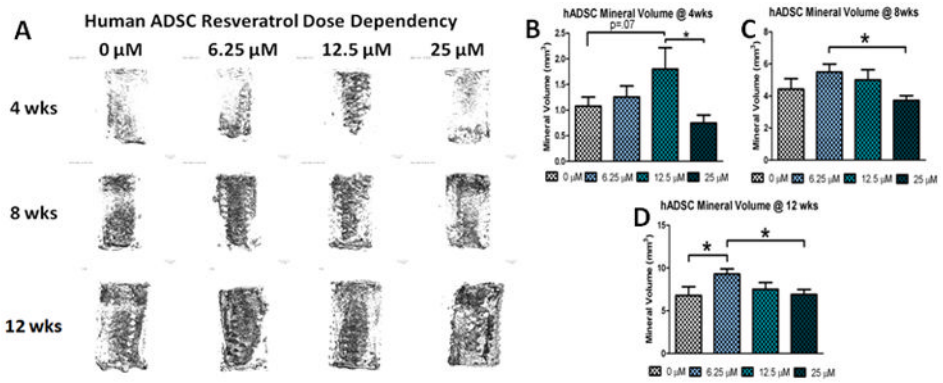

Figure 3.

The effect of resveratrol pre-treatment dosage on the 3-D osteogenic differentiation of hADSCs: A) Representative Micro-CT images of hADSC cell seeded constructs for different doses of resveratrol at 4, 8, and 12 weeks; Quantification of mineralized matrix after 4 weeks (B), 8 weeks (C) and 12 weeks (D) in osteogenic media. * = $p<.05$.

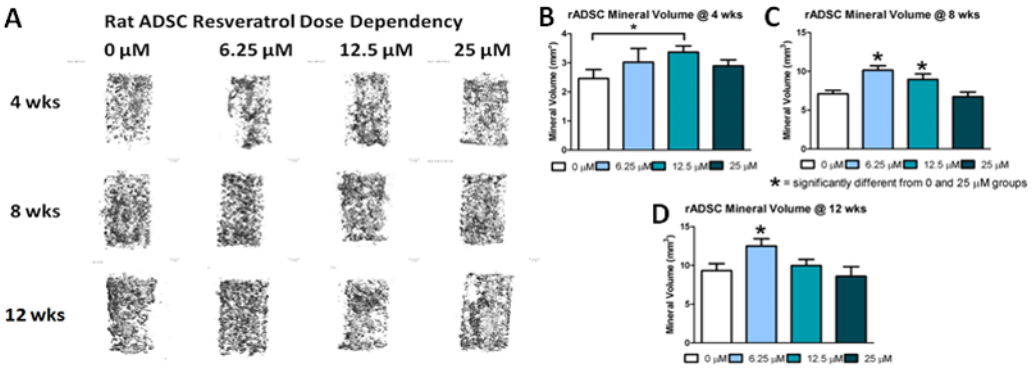

Figure 4.

The effect of resveratrol pre-treatment dosage on the 3-D osteogenic differentiation of rADSCs: A) Representative Micro-CT images of rADSC cell seeded constructs for different doses of resveratrol at 4, 8, and 12 weeks; Quantification of mineralized matrix after 4 weeks (B), 8 weeks (C) and 12 weeks (D) in osteogenic media. * = $p<.05$.

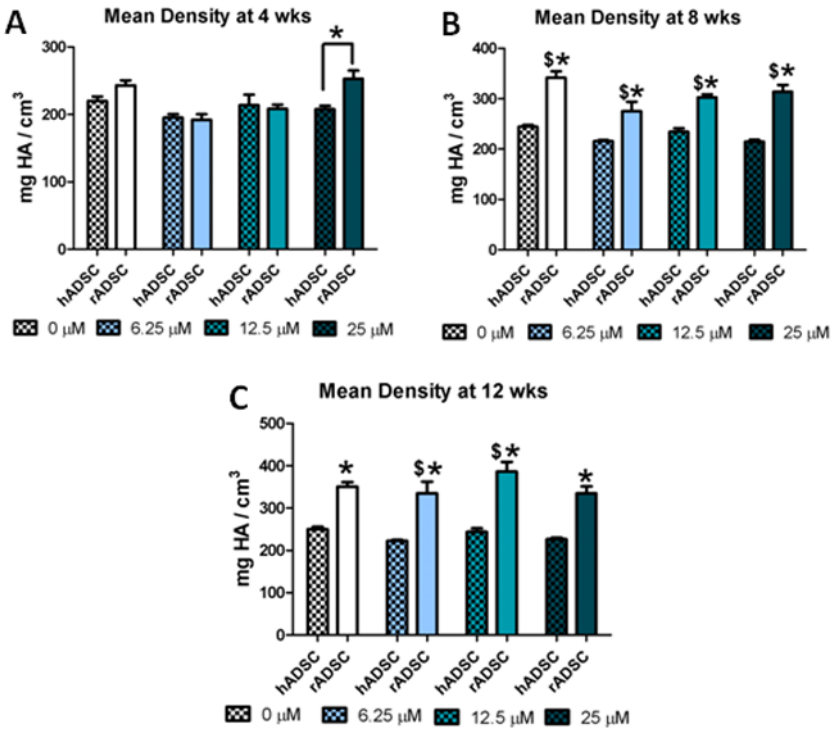

Figure 5.

Species effects on the mean density of mineralized matrix of rADSCs and hADSCs: average mean density of mineralized matrix for hADSCs and rADSCs at 4 weeks (A), 8 weeks (B), and 12 weeks (C). * = significantly different from other species at that time point ($p<.05$). $ = significantly different from the previous time point at that dose ($p<.05$).

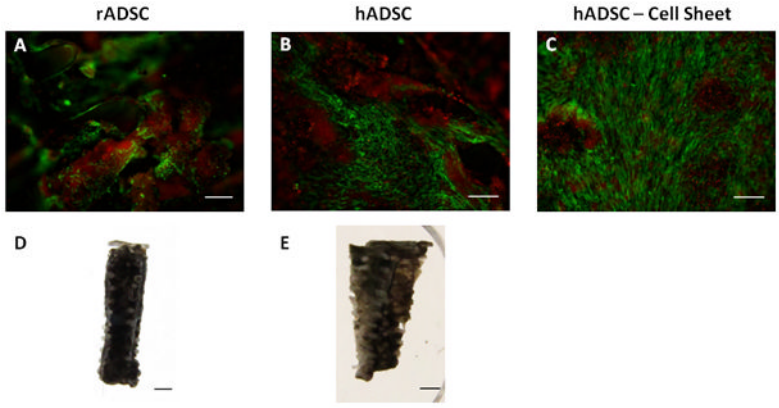

Figure 6.
Histological differences in the mineralized matrix of rADSCs and hADSCs: fluorescence imaging of rADSC (A) and hADSCs (B & C) after12 weeks of culture in osteogenic media (scale bar = .5 mm; green = cells, red = mineral). Von Kossa staining of rADSC (D) and hADSC (E) cell seeded constructs after 12 weeks of culture in osteogenic media (scale bar = 1 mm).

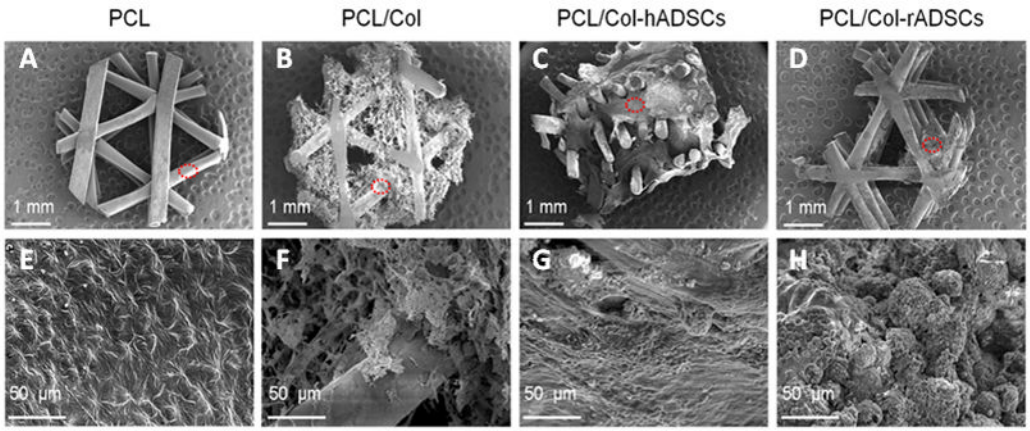

Figure 7.
Surface characterization of PCL/collagen scaffolds and mineralized matrix: Scanning electron microscope images of PCL (A&E), PCL/Col (B&F), PCL/Col-hADSCs (C&G), and PCL/Col-rADSCs (D&H). The red dot circle indicates the area of higher magnification, shown in the second row of this figure.

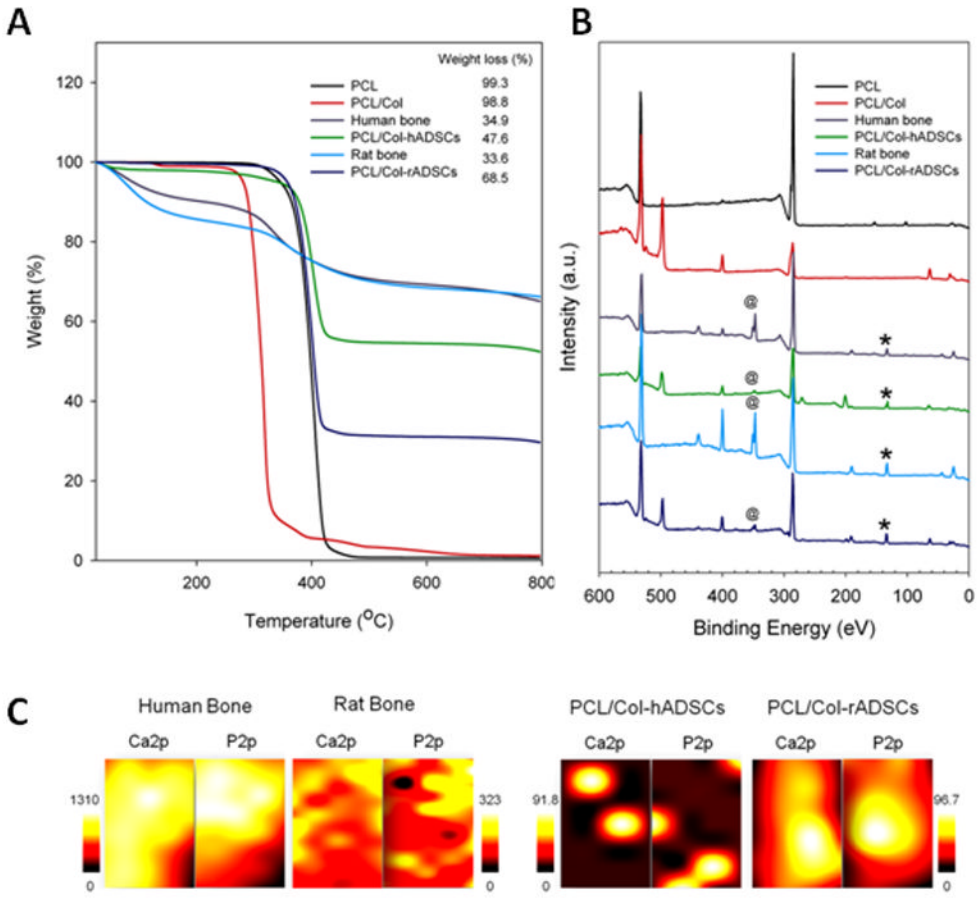

Figure 8.

Evaluation of the mineralized matrix and comparison to bone samples: A) TGA decomposition profiles of PCL, PCL/Col, human bone, PCL/Col-hADSCs, rat bone, and PCL/Clol-rADSCs under N_2 atmosphere; B) x-ray photoelectron spectroscopy (XPS) general survey spectra for PCL, PCL/Col, human bone, PCL/Col-hADSCs, rat bone, and PCL/Col-rADSCs (@ = Ca2p peak, * = P2p peak); C)XPS chemical mapping of Ca2p and P2p on human and rat bone (B) and PCL/Col-hADSCs and PCL/Col-rADSCs (Mapping area = 0.44 mm^2).